JOURNAL OF CATALYSIS 74, 266–274 (1982)

Kinetics and Rate Oscillations of the Oxidation of Propylene Oxide on Polycrystalline Silver

MICHAEL STOUKIDES AND COSTAS G. VAYENAS

Massachusetts Institute of Technology, Cambridge, Massachusetts 02139

Received July 13, 1981; revised November 19, 1981

The oxidation of propylene oxide on porous polycrystalline Ag films supported on stabilized zirconia was studied in a CSTR at temperatures between 250 and 400°C and atmospheric total pressure. The technique of solid electrolyte potentiometry (SEP) was used to monitor the chemical potential of oxygen adsorbed on the silver catalyst. The steady state kinetic and potentiometric results are consistent with a Langmuir–Hinshelwood mechanism. However over a wide range of temperature and gaseous composition both the reaction rate and the surface oxygen activity were found to exhibit self-sustained isothermal oscillatory behavior. Oxidation of propylene, ethylene, and ethylene oxide on the same surface under similar conditions does not produce oscillations. A possible cause for this phenomenon will be discussed.

INTRODUCTION

Unlike ethylene oxide production, the main routes for propylene oxide production are not based on direct catalytic oxidation of propylene, mainly because of the low conversions and selectivities to propylene oxide. The major industrial processes currently used for propylene oxide formation are the propylene-chlorohydrin and the "oxirane" process (*4*). Propylene oxide formation by direct oxidation of propylene on silver would be financially preferable if high yield and selectivity to propylene oxide could be achieved (*4, 5*).

Therefore, a large number of investigators have studied the optimal conditions for direct propylene oxidation (*3, 6–8*) as well as the promoting effect of various compounds including chlorinated hydrocarbons, CaO and BaO (*15, 7*).

Similarly to ethylene oxidation on silver part of the undesirable by-product CO_2 comes from the secondary oxidation of propylene oxide (*2, 9, 10, 20*). The kinetics and mechanism of the secondary oxidation of propylene oxide to CO_2 and H_2O is the subject of the present communication. Although an understanding of the mechanism of this reaction is necessary for the understanding of the overall propylene oxidation network, relatively few investigators have studied the propylene oxide oxidation separately (*2, 11, 20*).

Kaliberdo *et al.* (*2, 20*) studied the oxidation of propylene oxide on pure silver and on silver supported on various carriers. They found that on pure silver only CO_2 and water are produced below 420°C. Isomerization products including propionaldehyde, acetone, and acetaldehyde were found as products when a-Al_2O_3 and silicon carbide were used as carriers. Cant and Hall (*11*) studied the oxidation of ethylene and propylene labeled with deuterium as well as cooxidation of unlabeled olefins with the corresponding ^{14}C-labeled epoxides at temperatures 200–220°C. They found that in both instances most of the undesirable CO_2 originates from direct oxidation of the olefins and thus the reason for low selectivity of silver for propylene oxide formation is not primarily due to the instability of propylene oxide under reaction conditions.

In the present investigation a detailed study of the reaction kinetics is combined with simultaneous *in situ* measurement of the thermodynamic activity of oxygen adsorbed on the catalyst by using the tech-

0021-9517/82/040266-09$02.00/0

nique of solid electrolyte potentiometry (SEP). The technique originally proposed by C. Wagner (*1*) utilizes a solid electrolyte oxygen concentration cell with one electrode also serving as the catalyst for the reaction under study. It has already been used in conjunction with kinetic measurements to study the SO_2 oxidation on noble metals (*13*) as well as the oxidation of ethylene on silver (*14*) and on Pt (*17*). Similar solid electrolyte cells have been used for electrochemical enhancement of catalytic reaction rates including NO decomposition on Pt (*18*) and ethylene oxidation on silver (*19*).

Several catalytic oxidations have been found to exhibit rate oscillations on Pt and Ni (*21*). Solid electrolyte potentiometry has already been used to study and interprete the isothermal rate oscillations of ethylene oxidation on platinum (*22*).

EXPERIMENTAL METHODS

Catalyst and Apparatus

The apparatus and the reactor cell used have been described in detail in previous communications (*12, 14*). The porous silver catalyst film was deposited on the inside flat bottom of an 8% yttria stabilized zirconia tube. The superficial area of the tube is 2 cm^2 and the total catalyst surface area is approximately 2000 cm^2. The catalyst preparation and characterization have been described previously (*12*). A similar silver film served as a reference electrode and was deposited on the outside flat bottom of the zirconia tube. The reactor has been shown to behave as a CSTR for the flowrates employed in this study (*12, 17*).

Reactants were Matheson certified standards of propylene oxide in nitrogen and Matheson zero grade air. In order to maintain the partial pressure of either oxygen or propylene oxide constant the reactants could be further diluted in nitrogen. Reactants and products were analyzed by means of a Perkin Elmer Gas Chromatograph with a TC detector. A molecular sieve 5A column was used to separate N_2 and O_2. A Porapak Q column was used to separate air, CO_2, and propylene oxide. The CO_2 concentration in the effluent stream was also monitored using a Beckman 864 IR analyzer. The open circuit emf of the oxygen concentration cell was measured with a J. Fluke differential voltmeter. The correct performance of the cell was verified by introducing air-N_2 mixtures of known compositions and obtaining agreement within 1–2 mV with the Nernst equation

$$E = \frac{RT}{2F} \ln \left[\frac{P_{O_2}}{0.21}\right]^{1/2}. \quad (1)$$

Measurement of Oxygen Activity

Solid electrolyte potentiometry (SEP) was used to measure *in situ* the thermodynamic activity of oxygen on the silver catalyst film. It has been well established (*1, 12*) that the measured open circuit emf reflects the difference in chemical potential of oxygen adsorbed on the two silver electrodes

$$E = \frac{1}{4F}[\mu_{O_2}(\text{Ag, catalyst}) - \mu_{O_2}(\text{Ag, reference})]. \quad (2)$$

The chemical potential of oxygen adsorbed on the reference electrode which is in contact with air ($P_{O_2} \sim 0.21$ bar) is given by

$$\mu_{O_2}(\text{Ag reference}) = \mu_{O_2}{}^0(g) + \text{RT} \ln (0.21) \quad (3)$$

where $\mu_{O_2}{}^0(g)$ is the standard chemical potential of oxygen at the temperature of interest. The activity a_O of adsorbed oxygen can be defined by the equation

$$\mu_{O_2}(\text{catalyst}) = \mu_{O_2}{}^0(g) + RT \ln a_O{}^2. \quad (4)$$

Thus $a_O{}^2$ expresses the partial pressure of gaseous oxygen that would be in the thermodynamic equilibrium with oxygen adsorbed on the silver surface, if such an equilibrium were established. Therefore combining Eqs. (1), (2), and (4) a_O is given by

$$a_O = 0.21^{1/2} \exp \frac{2FE}{RT}. \quad (5)$$

The above equation is always valid irrespective of whether thermodynamic equilibrium is established between absorbed and gas phase oxygen or not. In the special case that thermodynamic equilibrium indeed exists between gaseous and adsorbed oxygen, then

$$a_O^2 = P_{O_2}. \quad (6)$$

RESULTS

Potentiometric Measurements

The low values of the open circuit emf during the reaction (−15 ~ −250 mV) show that in general $a_O^2 < P_{O_2}$. This implies that thermodynamic equilibrium is not established between gaseous oxygen and oxygen adsorbed on silver during reaction. The activity of oxygen was found to decrease as P_{PrO} increases by keeping the temperature and the pressure of oxygen constant. On the other hand a_O increases with increasing P_{O_2} and with increasing temperature.

Several functional forms were examined in order to describe the dependence of a_O on gas composition. It was found that the a_O measurements could be correlated in a satisfactory way by the expression

$$\frac{a_O}{P_{O_2}^{1/2} - a_O} = \frac{K}{P_{PrO}} + K'. \quad (7)$$

This is shown in Fig. 1. In Fig. 2 ln K is plotted vs temperature; K increases with temperature according to

$$K = 2.4 \times 10^3 \exp(-9600/T). \quad (8)$$

Kinetic Measurements

The kinetics were studied at temperatures between 240 and 390°C, propylene oxide partial pressures between 0.4 × 10^{-3} and 4.0 × 10^{-3} bar and oxygen partial pressures between 0.02 and 0.2 bar. External diffusional limitations were absent over the entire range of temperatures and gas compositions examined. This was verified by varying the flowrate and observing no change in the reaction rate and also by the fact that the rate of propylene oxide oxidation was found to be one to two orders of

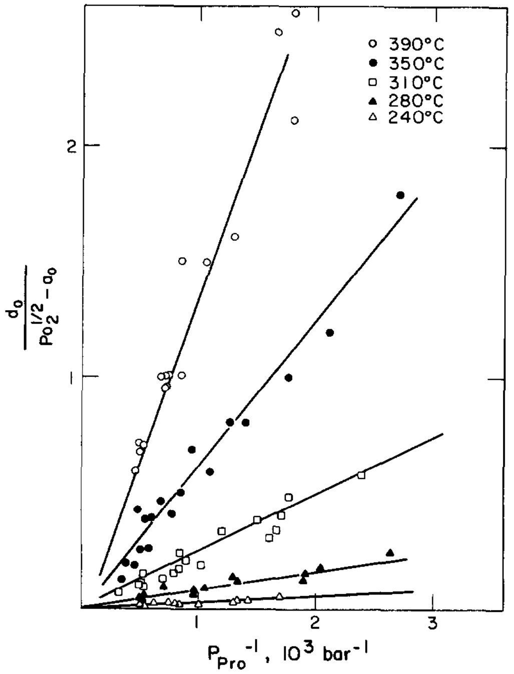

FIG. 1. Surface oxygen activity dependence on gas phase composition.

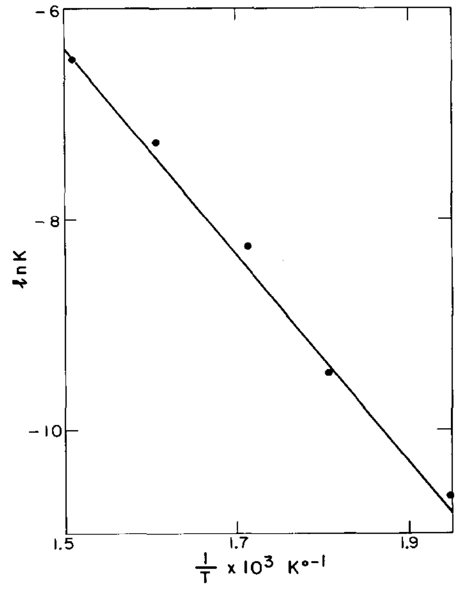

FIG. 2. Temperature dependence of K.

magnitude lower than the rates of ethylene and propylene oxidation (*14*, *16*) obtained with the same reactor and with similar flowrates. Diffusional effects inside the porous silver film were also negligible. This was verified by using different reactors with Ag films thicknesses between 3 and 10 μm and observing no difference (<2%) in the open circuit voltages measured for the same temperature and gas composition. Since the open circuit emf reflects the surface oxygen activity a_0 at the gas–metal–zirconia interline, this proves the absence of internal mass transfer limitations.

The rate of the reaction was calculated from the equation

$$r = F'[X_{\mathrm{Pro(Reactants)}} - X_{\mathrm{Pro(Products)}}] \quad (9)$$

where F' is the total molar flowrate and X is the mole fraction of propylene oxide.

The rate is shown in Fig. 3 as a function of the partial pressure of oxygen in the gas phase, P_{O_2} for various temperatures examined. The rate is zero order in oxygen at all temperatures. In Fig. 4a the rate is shown as a function of the partial pressure of propylene oxide P_{Pro}. The rate is close to first order with respect to P_{Pro} at the highest temperature (390°C) but this simple first order dependence disappears at lower temperatures.

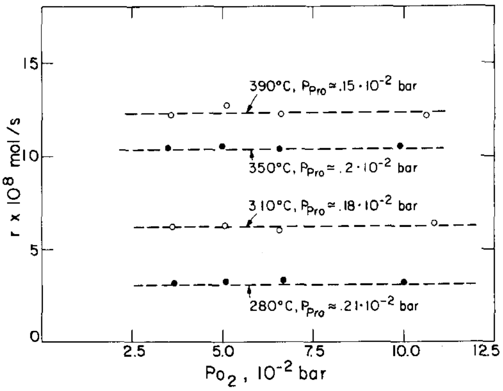

FIG. 3. Oxidation rate of propylene oxide vs P_{O}.

It was found that all the kinetic data could be expressed quite accurately by the

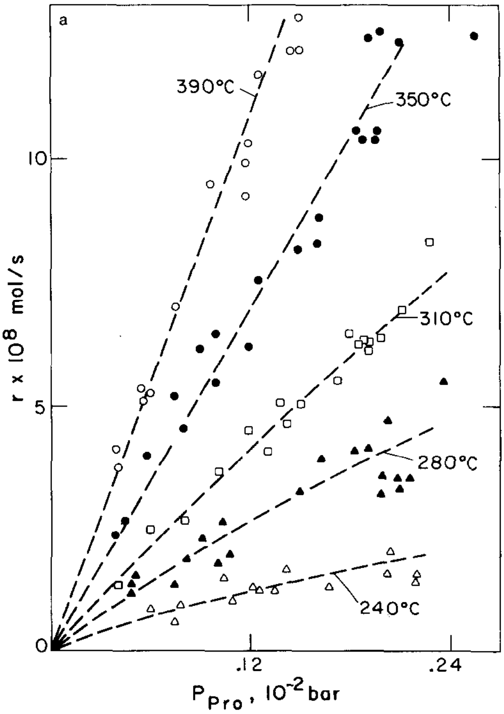

FIG. 4a. Oxidation rate vs the partial pressure of propylene oxide.

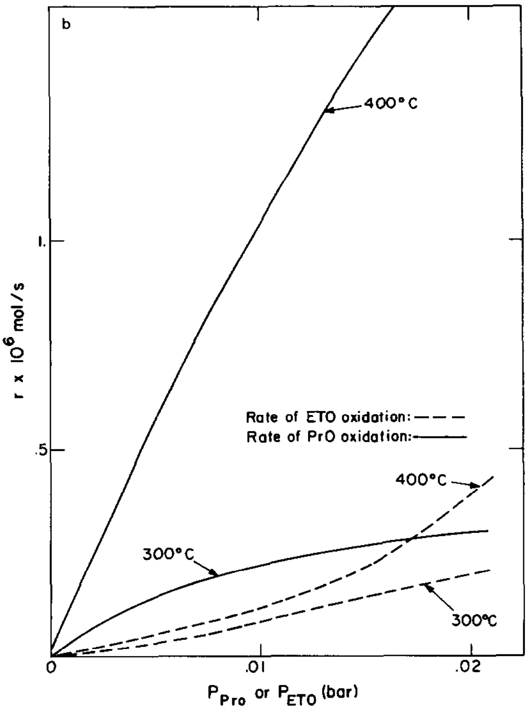

FIG. 4b. Comparison of the rates of ethylene oxide and propylene oxide oxidations at 300 and 400°C. Both rates are zero order in oxygen.

rate expression

$$r = K_R \frac{K_{Pro}P_{Pro}}{1 + K_{Pro}P_{Pro}} \qquad (10)$$

where r is given in moles/s and

$$K_R = 6.4 \exp\left(-\frac{19{,}000}{RT}\right) \text{ moles/s} \qquad (11)$$

and

$$K_{Pro} = 0.010 \exp\left(\frac{10{,}400}{RT}\right) \text{ bar}^{-1}. \qquad (12)$$

Propylene oxide oxidation is considerably faster than ethylene oxide oxidation on the same silver surface. This is shown in Fig. 4b where the rates of propylene oxide and ethylene oxide oxidation are compared at 300 and 400°C under identical conditions. Unlike ethylene oxide oxidation where both the kinetic and potentiometric results indicate the existence of significant amounts of chemisorbed dimer (*12*), the steady-state behavior of propylene oxide oxidation [Eqs. (7) and (10)] suggests that propylene oxide oxidation at steady state proceeds mainly via adsorbed monomer.

Rate and Oxygen Activity Oscillations

Over a wide range of temperature, space velocity, and gas composition the rate of CO_2 production as well as the surface oxygen activity exhibit oscillatory behavior (Fig. 5). However since the amplitude of the rate oscillations is typically less than 15% of the steady state rate, Eq. (10) can be used as an estimate of the average rate of CO_2 formation in the oscillatory region as well.

The period and amplitude of the oscillations were found to depend on temperature, residence time, as well as on gas composition. The oscillations were often quite complex. Typical periods were between 3 and 60 min. The rate of CO_2 production and the surface oxygen activity oscillate simultaneously, with increasing surface oxygen ac-

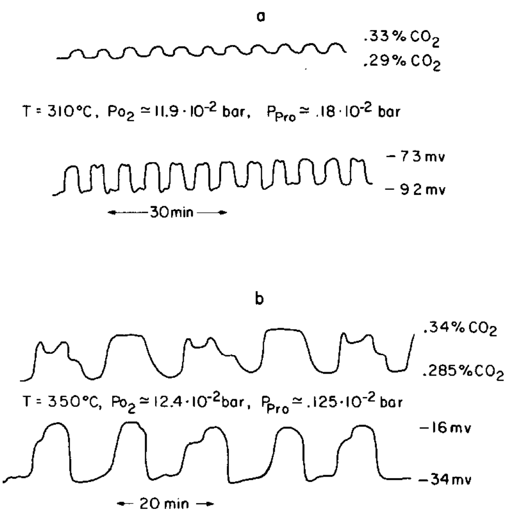

FIG. 5. Typical rate and emf oscillations.

tivity generally corresponding to increasing rate (Fig. 5). Typical amplitudes were 2–20 mV for the emf and up to 0.5×10^{-3} bar for the partial pressure of CO_2 in the effluent stream. As shown in Fig. 5 and in the subsequent figures the details of the rate oscillation waveform frequently differ from those of the oxygen activity oscillation.

There are no specific temperature limits between which oscillations occur. Oscillatory phenomena were observed from 240°C, the lowest temperature studied, and over the entire range of temperatures examined. The effect of temperature at constant gas composition and residence time is shown in Fig. 6. In general as temperature increases both the period and the amplitude of the oscillations decrease. As stated above rate and oxygen activity were always found to oscillate in phase. The apparent phase lag of Figs. 6 and 7 is due to the dead time required for the reactor effluent to reach the IR CO_2 Analyzer and also due to the displacement of the pens of the strip chart recorder.

The effect of the residence time on the frequency and amplitude of the oscillations is shown in Fig. 7. By increasing the total molar flowrate at constant temperature and gas composition, both the period and the amplitude of the oscillation decrease.

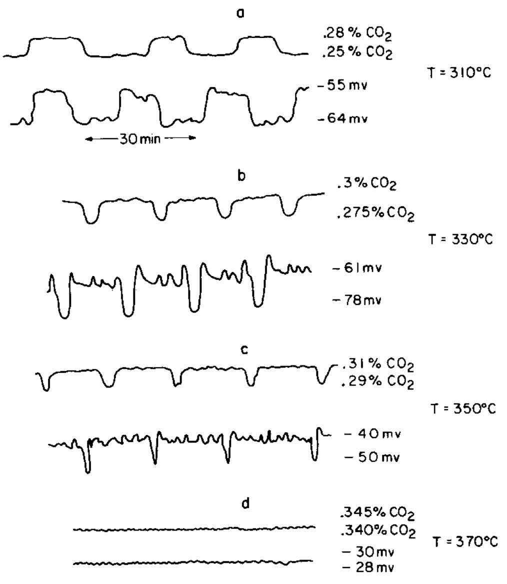

FIG. 6. Temperature effect on rate and emf oscillations at constant flowrate and gas composition. There is no real phase lag as discussed in the text.

Table 1 shows the dependence of the period and amplitude of oscillations on the partial pressure of oxygen in the gas phase

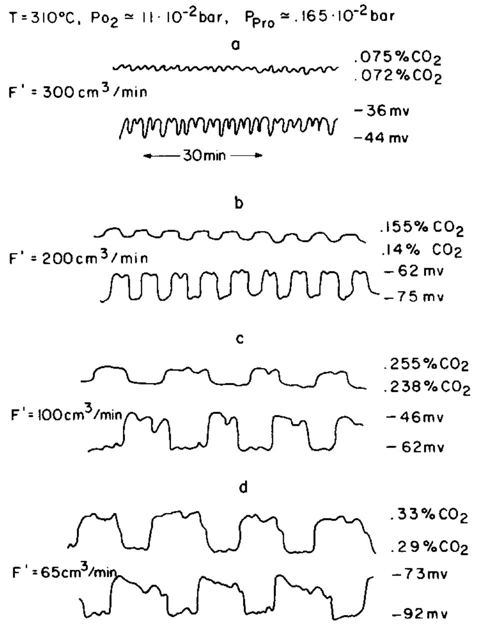

FIG. 7. Effect of residence time at constant temperature and gas composition. There is no real phase lag as discussed in the text.

TABLE 1

Effect of P_{O_2} on the Period and Amplitude of Reaction Rate Oscillations

	$T = 350°C$, P_{O_2} (bar)	$F' = 100\ cm^3/min$ Period τ (min)	$P_{Pro} \simeq 0.00155$ bar Amplitude (%)
a.	0.040	30	6.5
	0.055	10	3.1
	0.155	7.5	2.3
b.	$T = 350°C$, P_{O_2} (bar)	$F' = 205\ cm^3/min$ Period τ (min)	$P_{Pro} \simeq 0.002$ bar Amplitude (%)
	0.031	17	3.2
	0.053	12	1.3
	0.112	8.5	0.8

for constant temperature, P_{Pro} and residence time. The amplitude is expressed as percentage deviation from the average rate. The period decreases as P_{O_2} increases. No specific correlation was found between the period τ_c or the amplitude of the oscillations and the pressure of propylene oxide P_{Pro}. It was found however that for each temperature there is a specific range of P_{Pro}/P_{O_2} within which oscillations occur. This is shown in Fig. 8. Such a range was not found for the oxygen activity at any temperature.

The oscillations were isothermal. This was verified by attaching a thermocouple directly to the catalyst film and measuring a constant temperature within 1°C. This is expected since the heat released due to the reaction rate is negligible because of the very low partial pressures of propylene oxide employed in this study.

DISCUSSION

Steady-State Kinetics

The mechanism of the catalytic oxidation of propylene oxide can be now discussed on the basis of the reaction kinetics and the information provided by the solid electrolyte aided surface oxygen activity measurements. A satisfactory reaction mechanism should account not only for the kinetics [Eqs. (10), (11), (12)] but also for the surface oxygen activity behavior [Eqs. (7), (8)]. A reaction model explaining both kinetic and potentiometric observations in a semiquantitative manner is presented below.

We assume that propylene oxide and oxygen adsorb on different surface sites of the silver surface. Although more than one type of adsorbed oxygen have been reported to exist on silver we will consider only atomic oxygen in this study. This does not imply that atomic oxygen is the only form of oxygen adsorbed on silver. But we neglect in the present time the existence of molecular oxygen since we consider the atomic type responsible for the oxidation of propylene oxide.

We will assume a Langmuir type adsorption for both atomic oxygen and propylene oxide. If thermodynamic equilibrium is established between surface and gaseous propylene oxide the coverage θ_{Pro} is given by the equation

$$\theta_{Pro} = \frac{K_{Pro}P_{Pro}}{1 + K_{Pro}P_{Pro}} \tag{13}$$

where K_{Pro} is the adsorption coefficient of propylene oxide.

In the case of adsorbed atomic oxygen because of the definition of surface oxygen activity a_O [Eq. (4)] and the Langmuir adsorption assumption it follows that

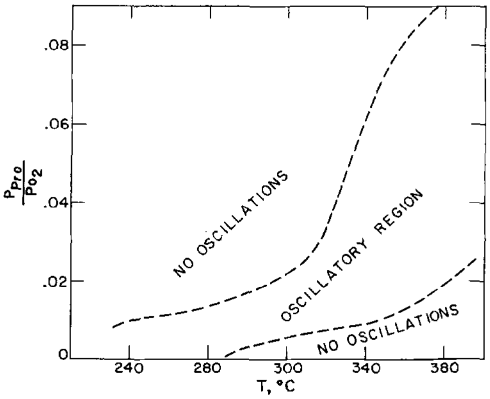

FIG. 8. Temperature effect on the upper and lower propylene oxide/oxygen limits for oscillations.

$$\theta_O = \frac{K_O a_O}{1 + K_O a_O}. \tag{14}$$

Note that Eq. (14) relates two intrinsic surface properties and is valid whether or not equilibrium with the gas phase exists (*12, 14, 17*).

On the basis of the above assumptions and considering the reaction to take place between adsorbed propylene oxide and adsorbed atomic oxygen one can write the rate expression as

$$r = K_R \theta_{Pro} \theta_O. \tag{15}$$

Substituting the values of θ_O, θ_{Pro} from Eqs. (14) and (13) one obtains

$$r = K_R \frac{K_{Pro} P_{Pro}}{1 + K_{Pro} P_{Pro}} \frac{K_O a_O}{1 + K_O a_O} \tag{16}$$

which reduces to the experimental expression (10) if $K_O a_O \gg 1$.

Since K_{Pro} is interpreted as the adsorption coefficient of propylene oxide on silver one can calculate from Eq. (12) an enthalpy of adsorption

$$\Delta H_{Pro} = -43.5 \text{ KJ/mol} \tag{17}$$

and an entropy of adsorption

$$\Delta S_{Pro} = -38.2 \text{ J/mol} \cdot \text{K}. \tag{18}$$

The surface oxygen activity behavior can be explained now by considering a steady state mass balance for adsorbed atomic oxygen

$$K_{ad} P_{O_2}{}^{1/2}(1 - \theta_O) = K_d \theta_O + K_R \theta_{Pro} \theta_O. \tag{19}$$

The left-hand side term corresponds to atomic oxygen adsorption and the right-hand side terms correspond to desorption of atomic oxygen and surface reaction, respectively. Experimental justification for the first order adsorption and desorption terms has been provided in a previous communication (*12*).

Taking into account Eqs. (13) and (14) and dividing Eq. (19) by $K_{ad}(1 - \theta_O)$ one obtains:

$$P_{O_2}{}^{1/2} - a_O = \frac{K_R}{K_D} a_O \left(\frac{K_{Pro} P_{Pro}}{1 + K_{Pro} P_{Pro}} \right). \tag{20}$$

Dividing Eq. (20) by a_O and taking the reciprocal of both terms one obtains

$$\frac{a_O}{P_{O_2}{}^{1/2} - a_O} = \frac{K_D}{K_R} + \frac{K_D}{K_R K_{Pro}} \frac{1}{P_{Pro}} \tag{21}$$

which describes the experimental observations (7) with

$$K = \frac{K_D}{K_R K_{Pro}} \quad \text{and} \quad K' = \frac{K_D}{K_R}.$$

Furthermore from the experimental values of K, K_R, K_{Pro} [Eqs. (8), (10), (11)] one can calculate K_D, the desorption coefficient of atomic oxygen

$$K_D = 155 \exp\left(-\frac{27500}{RT}\right) \text{ moles/s.}$$

The activation energy of 27.5 kcal/mole found for K_D is in good agreement with previous work (*9, 12*).

The above model explains the steady-state behavior in a quantitative way but it fails to explain the oscillatory phenomena that were observed. Nevertheless since the amplitude of the oscillations is typically 2–15%, Eqs. (7) and (10) can be used approximately in both regions.

The origin of the limit cycles is not clear. Rate oscillations have not been reported previously for silver catalyzed oxidations. Oxidation of ethylene, propylene, and ethylene oxide on the same silver surface and under identical temperature, space velocity and air–fuel ratio conditions did not give rise to oscillations. It thus appears that the oscillations are related specifically to the nature of chemisorbed propylene oxide. This is also supported by the lack of any correlation between the limits of oscillatory behavior and the surface oxygen activity. This makes the SEP measurements much less useful for interpreting the oscillations than in the case of ethylene oxidation on Pt (*22*) where the periodic behavior was due to the peculiarities of the platinum–oxygen interaction, i.e., surface platinum oxide formation. The lack of any correlation between surface oxygen activity and the limits of oscillatory behavior as well as the fact that ethylene, ethylene oxide, and propylene oxidation exhibit steady-state behavior over the same range of surface oxygen activity values seems to indicate that periodic oxidation-reduction of the surface is not the source of the oscillations.

Very little is known about the exact nature of propylene oxide chemisorption on silver. There is evidence of isomerization to acrolein and for polymer formation (*6*). Formation of a surface polymeric structure has also been observed during propylene oxidation on silver (*24*). It would appear possible, if not likely, that the rate oscillations are related to the ability of chemisorbed propylene oxide to form relatively stable intermediates or polymeric structures. Thus chemisorbed monomer could account for the steady-state kinetics discussed above whereas the superimposed fluctuations on the rate could originate from periodic formation and combustion of surface polymeric residues. A mathematical model based on this assumption and describing the oscillations in a qualitative manner will be presented in a later communication (*16*).

In summary, although the kinetic and potentiometric results of propylene oxide oxidation on silver can be interpreted within the framework of a simple Langmuir–Hinshelwood mechanism with two types of adsorption sites, further work is required to interprete the observed rate and oxygen activity oscillations. It is likely that the oscillations are related to the ability of propylene oxide to form polymeric structures. Understanding the origin of the oscillations may be quite important in obtaining a better picture of the oxidation of propylene on silver and devising methods to improve the selectivity to propylene oxide. We note that propylene oxide oxidaton is the first known reaction which exhibits periodic behavior on silver.

ACKNOWLEDGMENTS

This research was supported under NSF Grant CPE-8009436 and under the MIT J. R. Mares career development professorship Grant.

REFERENCES

1. Wagner, C., *Adv. Catal.* **21,** 323 (1970).
2. Kaliberdo, L. M., Vaabel, A. S., and Torgasheva, A. A., *Kinet. Katal.* **8,** 105 (1967).
3. Manara, G., and Parravano, G., *J. Catal.* **32,** 72 (1974).
4. Kuhn, W., *Chem. Eng. Prog.* **76** (1980).
5. Sherwood, P., *Chem Ind.* **87,** 764 (1962).
6. Freriks, I. C., Bouwman, R., and Geenen, P. V., *J. Catal.* **65,** 311 (1980).
7. Kaliberdo, L. M., *et al., Kinet. Katal.* **8,** 463 (1967)..
8. Inui, T., Ueda, T., Suehio, M., and Shingu, H., *J. Chem. Soc. Faraday Trans.* **74,** 2430 (1978).
9. Kilty, R. A., and Sachtler, W. M. H., *Cat. Rev.-Sci. Eng.* **10,** 1974.
10. Voge, H. H., and Adams, C. R., *Adv. Catal.* **17,** 154 (1967).
11. Cant, N. W., and Hall, W. K., *J. Catal.* **52,** 81 (1978).
12. Stoukides, M., and Vayenas, C. G., *J. Catal.* **64,** 18 (1980).
13. Vayenas, C., and Saltsburg, H., *J. Catal.* **57,** 926 (1979).
14. Stoukides, M., and Vayenas, C. G., *J. Catal.* **69,** 18 (1981).
15. Kaliberdo, L. M., and Zhukova, G. G., *Izv. Nauch.-Issled. Inst. Neft-Uglekhim. Sin. Irkutsk. Univ.* **9,** 136 (1967).
16. Stoukides, M., and Vayenas, C. G., in preparation.
17. Vayenas, C. G., Lee, B., and Michaels, J., *J. Catal.* **66,** 34 (1980).
18. Pancharatnam, S., Huggins, R. A., and Mason, D. M., *J. Electrochem. Soc.* **122,** 869 (1975).
19. Stoukides, M., and Vayenas, C. G., *J. Catal.* **70,** 137 (1981).
20. Vaabel, A. S., Torgasheva, A. A., and Kaliberdo, L. M., *Kinet. Katal.* **7,** 826 (1966).
21. Sheintuch, M., and Schmitz, R., *Catal. Rev. Sci. Eng.* **15,** 1977.
22. Vayenas, C. G., Georgakis, C., Michaels, J., and Tormo, J., *J. Catal.* **67,** 348 (1981).
23. Twigg, G. H., *Proc. R. Soc. A* **188,** 92 (1946).
24. Kobayashi, M., *Canad. J. Chem. Eng.* **58,** 588 (1980).